Design and Operation of an Electromagnetically Guided Elevator Test Bench

Benedikt Schmülling, Rüdiger Appunn, Ferdinand Wikullil, and Kay Hameyer
Institute of Electrical Machines, RWTH Aachen University,
Schinkelstr. 4, D-52056 Aachen, Germany
Tel: +49-241-80-97667 – Fax: +49-241-80-92270 – e-mail: benedikt.schmuelling@iem.rwth-aachen.de

Topics: 41, 44

1. Introduction

Optimization of vertical passenger transportation systems is gaining importance, since more and more high-rise buildings occur in China or Arabia, for example. These buildings make high demands on their passenger transportation systems, since the height, and with it the number of floors, obtains new maxima every year. Examples are the Taipei Financial Center in Taiwan, the Petronas Towers in Malaysia, and the Burj Dubai in the United Arab Emirates, which is still under construction. In this sense, conventional elevators with mechanical guiding systems come to their application limitations due to the very high requirements of these buildings. An improvement of the operational behaviour of such high elevator systems can be achieved by using electromagnetic guides instead of slide or roller guides.

One benefit of electromagnetic guideways is the wear-free operation. In addition, these guideways have no consumption of lubricants, a further advantage compared to mechanical guideways.

Due to the frictionless operation, the elevator can be operated at a higher speed when compared to conventional systems. However, the main advantage is the possibility to control the ride comfort by adjusting the damping rate of the guiding system. The ride comfort depends on vibration and noise caused by misalignment and misconnection of the guide rail. This topic and the opportunity to improve the convenience are presented in literature, for example in [1]. The active control of the damping rate requires a closed loop system.

The presented work describes and explains the design of an elevator test bench equipped with electromagnetic guidings for the elevator car. Furthermore, the operational performance is measured and evaluated.

2. Layout of the Elevator Test Bench

The elevator test bench presented consists of an elevator shaft, an elevator car, and a rope with counterbalance as propulsion device. Sensor electronics and power converters of the guiding system are placed within the elevator car (Fig 1).

2.1. The Electromagnets

The guiding system consists of four electromagnets in the so called ω ("omega")-shape. Fig. 2 depicts one of these magnets. It consists of a three-legged laminated iron yoke, mounted with permanent magnets on the outer pole surfaces, and coils around the lateral legs. The operation

Figure 1: Electromagnetically guided elevator test bench.

of this electromagnet is based on the superposition of a permanent magnet flux with electrically excited fluxes [1],[2]. The analytical calculation of the electromagnet's fluxes is based on the method of the magnetic equivalent circuit. Herewith, the design of the magnet is performed. A numerical analysis of the electromagnet's fluxes (applying the Institute of Electrical Machines in-house FE-software package iMOOSE) verifies the analytical design method employed. In contrast to U-shaped actuators, the actuator is able to produce pulling forces in three directions. Table 1 shows the parameter of the ω-actuator.

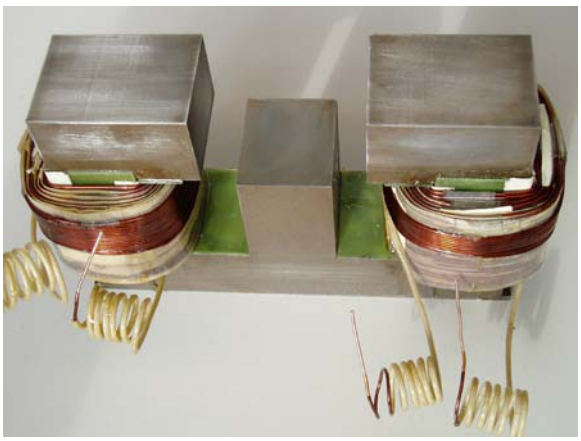

Figure 2: Electromagnet in ω-shape.

Table 1: Parameter of the ω-actuator.

class	parameter	symbol	value
iron yoke	pole lenght x	l_{Px}	50mm
	pole width x	b_{Px}	39mm
	pole face x	$A_x = b_{Px} \cdot l_{Px}$	$1.95 \cdot 10^3 \text{mm}^2$
	pole lenght y	b_{Py}	50mm
	pole width y	b_{Py}	42mm
	pole face y	$A_y = b_{Py} \cdot l_{Py}$	$2.10 \cdot 10^3 \text{mm}^2$
permanent magnet	height	h_{PM}	3mm
	remanence	B_r	1.22T
	coercivity	H_c	915kA/m
excitation winding	windings	w	250
	resistance	R	0.6 Ω
	inductance at working point	L	20mH

2.2. The DC/DC –Converters

Each coil of the electromagnets is driven by one DC/DC-Converter. The applied DC/DC-converters are well analysed for the use as electromagnet driver due to their implementation to other magnetically levitated vehicles before [3]. Fig. 3 presents two DC/DC-converters on a plug-in unit of the elevator test bench.

2.3. The Elevator Car

The elevator car is composed of an aluminium chassis, where the electronic devices are modularly integrated. Fig. 4 shows the front side of the elevator car inserted in the elevator shaft. The forefront of the plug-in units containing the DC/DC-converters and the peripheral electronics can be seen in this figure.

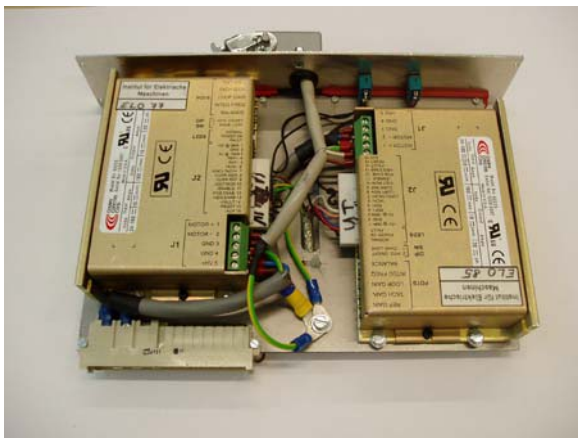

Figure 3: DC-converter plug-in unit.

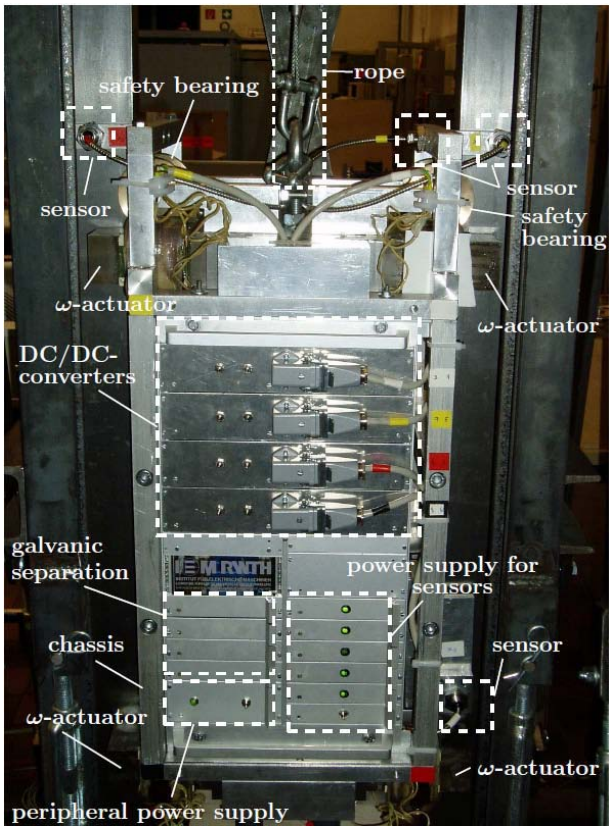

Figure 4: Elevator car of the test bench.

The stiffness of the chassis is quite high (the compliance is nearly zero); a deformation due to the electromagnetic forces of the actuating electromagnets is not expected. Hence, the measuring of five local positions is sufficient for a complete position estimation of the five degrees of freedom.

The electromagnets are mounted on two opposite edges of roof and floor of the elevator car in a so called symmetrical topology (similar to diagonal topology in [2]). Benefit of this topology is the low power consumption of the electromagnets since the uncontrolled suspension of the elevator car is in an unstable equilibrium when it is running without load.

2.4. Position Sensors

Five position sensors are required to completely detect the position of the elevator car in the shaft. Therefore, five eddy current sensors are mounted to the linear guiding system to measure the distance between the electromagnets and their return yokes.

2.5. The Control Section

The controller is established on an external digital signal processor unit. The subsequently adjustment of control parameters as well as the acquisition of sensor and control signals is possible by a computer based user interface.

2.6. Block scheme of the test bench

The complete block-scheme representation of the test-bench can be seen in Fig. 5. The signal-flow from the position vector **q** to the vector of magnetic forces $\mathbf{f_m}$ is presented. Airgap heights are measured with eddy current sensors. The analog signal is then filtered by an

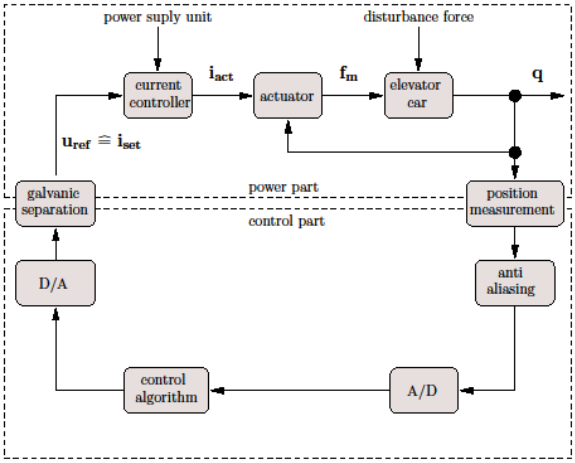

Figure 5: Block scheme representation of the full system.

antialiasing algorithm. After A/D transformation the designed control algorithm is used. The signal is transformed back by a D/A transformation. A galvanic separation between control and power part of the test bench is ensured by using an optocoupler. The reference voltage is the input signal for the current controllers of the DC/DC-converters. The output currents drive the coils of the actuators. Finally electromagnetic forces act on the elevator car. The feedback of the position vector **q** symbolizes the dependency of the electromagnetic force from the air gap height.

3. DOF-Control

The control method employed is the so called DOF (degree of freedom)-control [3],[4]. A benefit of this method compared to a simple air gap control (i.e. every single air gap height is controlled separately) is higher system stability, against the background of large manufacturing tolerances in high elevator shafts. The position vector is

$$\mathbf{q} = (x \quad y \quad \alpha \quad \beta \quad \gamma)^T . \qquad (1)$$

Each component of the **q** is separately controlled by a PID controller. For the design of this controller the method of pole placement [5] is applied to the state space system of the respective DOF.

4. Operation

The operation of the electromagnetically guided elevator car is verified by several test runs. Different load cases such as force impacts on the elevator car's wall and force steps due to unbalanced goods are analyzed.

4.1. Spatial displacement

Fig. 6 depicts a force impulse of 100N in x-direction on the elevator car. The spectrum of the impulse can be seen in Fig. 7. The resulting spatial displacement is shown in Fig. 8. After a short oscillation with a maximum of 0.09mm the elevator car returns to its working point $\mathbf{q}_0$. The compliance characteristic of DOF x is presented in Fig. 9. The maximum compliance occurs at an angular frequency of 60Hz. The reciprocal value of the maximum compliance is the minimum stiffness. This is a common quantity for the comparison of magnetically levitated vehicles. In Table 2 the minimum stiffness for all components of the spatial position vector **q** is specified.

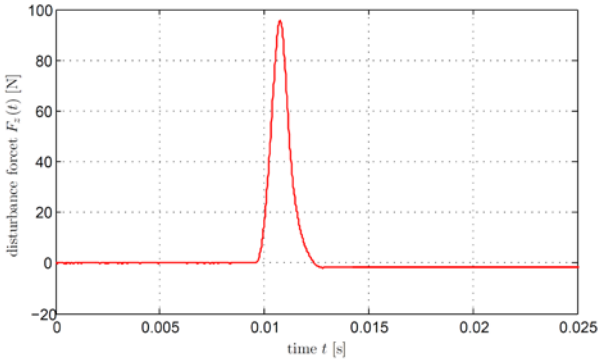

Figure 6: Force impulse in x direction.

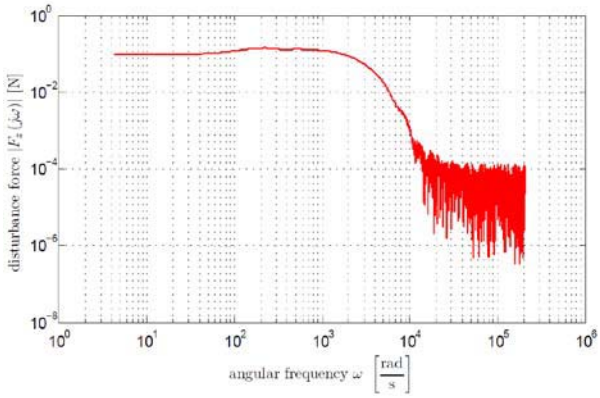

Figure 7: Spectrum of the force impulse.

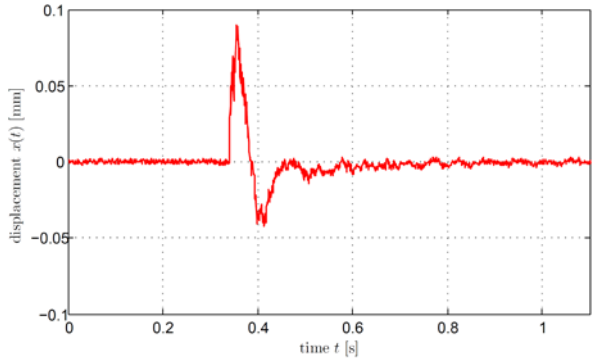

Figure 8: Position error of the controlled system in x-direction.

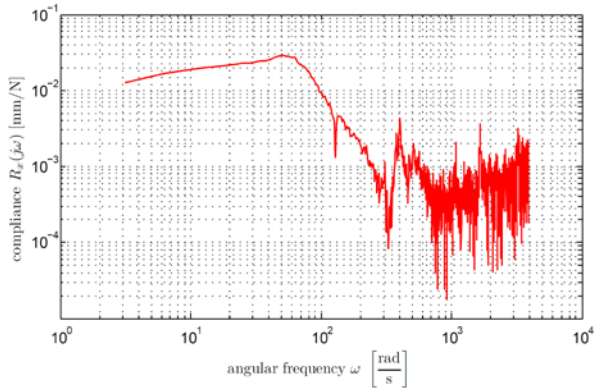

Figure 9: Compliance of the controlled system in x-direction.

Table 2: Simulated and measured values for stiffness of all five DOF.

DOF	minimum stiffness
x	$63.5\frac{N}{\mu m}$
y	$23.0\frac{N}{\mu m}$
α	$1.6\frac{kNm}{rad}$
β	$3.6\frac{kNm}{rad}$
γ	$2.0\frac{kNm}{rad}$

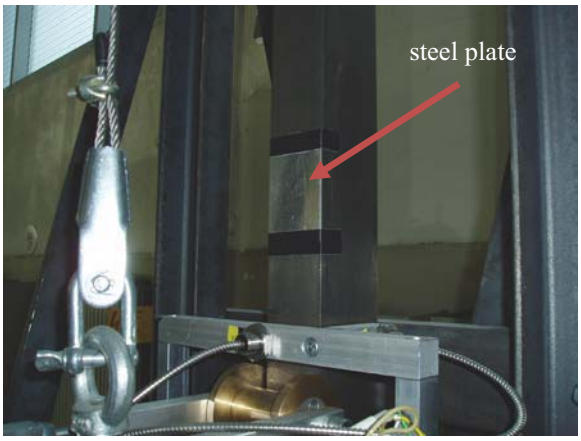

Figure 10: Surfaced defect on guide rail simulated by a steel plate.

4.2. Airgap variation

Surface defects on the guide rails resulting from oscillations in very high buildings, lead to variations in the airgap length. Herewith, a variation of the airgap reluctance follows. Nonetheless, a sufficient operation of the elevator system must be ensured. A thin steel plate is attached consecutively to one guide rail, resulting in reduced airgaps in y-direction (Fig. 10). Fig. 11 and 12 show the DOF y and α during a transit through these areas. Small deviations from working point can be seen but the control system keeps the elevator car in the equilibrium. The functionality of the control system is proven.

5. Conclusion

The elevator test bench constructed is well running and still part of several measurements and optimization developments. However, the test runs accomplished show a good performance with respect to robustness and power consumption. As expected, the average current value in the electromagnets' coils is zero. A detailed description of the elevator setup is presented in this paper. Measurement results form a force impact and the transit through areas with reduced airgaps are given. The results verify the design process and proof the functionality of the electromagnetic guiding system .

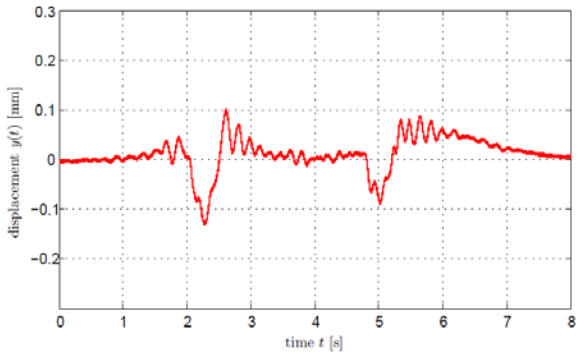

Figure 11: DOF y during transit through areas with reduced airgaps in y-direction.

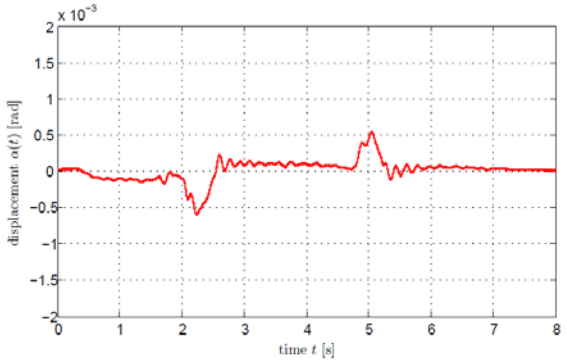

Figure 12: DOF α during transit through areas with reduced airgaps in y-direction.

References

[1] Morishita, M., Akashi, M., "Electromagnetic Non-contact Guide System for Elevator Cars," The Third International Symposium on Linear Drives for Industry Applications, pages 416-419, LDIA, Nagano, Japan, October 2001.

[2] Schmülling, B., Leßmann, M., van der Giet, M., Hameyer, K., "Proposals for the use of Magnetic Guideways for Vertical Transportation Systems," IJEET International Journal of Electrical Engineering in Transportation, 4(1): 9-13, 2008.

[3] Van Goethem, J., Henneberger, G., "Design and Implementation of a Levitation-Controller for a Magnetic Levitation Conveyor Vehicle," 8th Inter-national Symposium on Magnetic Bearing, pages 139-143, Mito, Japan, August 2002.

[4] Schmidt, A., Brecher, C., Possel-Dölken, F. "Novel Linear Magnetic Bearings for Feed Axes with Direct Drives," International Conference on Smart Machining Systems at the National Institute for Standards and Technology (NIST), Gaithersburg, MD, USA, March 13-15, 2007.

[5] Ghersin, A. S., Sánchez Peña, R. S., "LPV Control of a 6-DOF Vehicle," IEEE Transactions on Control Systems Technology, 10(6): 883 - 887, November 2002.